Quantum dot lasers grown on (001) Si substrate for integration with amorphous Si waveguides

Yating Wan[1], Qiang Li[1], Alan Y. Liu[2], Yu Geng[1], Justin Norman[2], Weng W Chow[3], Arthur C. Gossard[2,4], John E. Bowers[2,4], Evelyn L. Hu[5], and Kei May Lau[1]

1 Department of Electronic and Computer Engineering, Hong Kong University of Science and Technology, Clear Water Bay, Kowloon, Hong Kong

2 Materials Department, University of California Santa Barbara, Santa Barbara, California 93106, USA

3 Sandia National Laboratories, Albuquerque, NM 87185-1086, USA

4 Department of Electrical and Computer Engineering, University of California Santa Barbara, Santa Barbara, California 93106, USA

5 School of Engineering and Applied Sciences, Harvard University, Cambridge, MA 02138, USA

eekmlau@ust.hk

Abstract: Heteroepitaxially grown InAs quantum dot lasers were demonstrated on (001) Si under continuous-wave optical pumping with low thresholds (down to 35 μW). The feasibility of integrating active and passive devices through electrical injection was analyzed.

OCIS codes: (230.5590) Quantum-well, -wire and -dot devices; (140.5960) Semiconductor lasers; (140.3948) Microcavity devices; (160.3130) Integrated optics materials

1. Introduction

Integration of direct band-gap III–V materials with the dominant complementary metal oxide-semiconductor (CMOS) technology is promising to help relieve data exchange bottlenecks encountered at both intra-chip and inter-chip scales [1]. By exploiting the capability of quantum dots (QDs) to withstand non-radiative defects, heteroepitaxial growth of III-V on Si may allow low-cost and high-yield manufacturing [2, 3], higher temperature operation and reduced sensitivity to reflections [4]. However, the reported state-of-art lasers grown on Si rely on thick epitaxial layers that nearly exceed the critical thickness, and the offcut Si substrate that hampers their full compatibility with the mainstream CMOS technology, possessing thresholds on the order of 10 mA. More attention is needed to address the issues associated with power dissipation and process integration compatibility.

In this work, we are developing high-performance QD lasers directly grown on exact (001) silicon substrates. Under continuous optical pumping, room temperature lasing was achieved in 4-μm diameter microdisks with excellent temperature characteristics of 105 K in the 1.3-μm wavelength range. Subwavelength lasing in micro-disk lasers as small as 1 μm in diameter was demonstrated in the 1.2-μm wavelength range, with low thresholds down to 35 μW at 10 K. To explore the full extension of the optically pumped micro-disk structure towards practical electrically injected laser configurations in a monolithic integration platform, we further combine InAs quantum dots gain elements with index matched amorphous silicon waveguide devices through evanescent coupling. The feasibility of integrating active and passive devices was analyzed and simulated.

2. Experiments and results

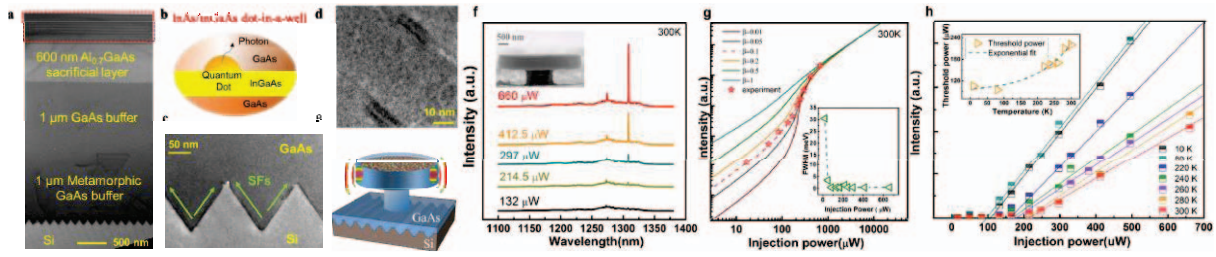

Fig. 1. (a) TEM image of the epi-layer structure; (b) schematic of the DWELL; (c) TEM of the GaAs/Si hetero-interface; (d) TEM of the QDs; (e) schematic of the mciro-disk (f) μPL spectra of the 4-μm-diameter microdisk laser at different pump powers; (g) L-L curve in the log-log scale, inset: linewidth narrowing; (h) L-L curves at different temperatures, inset: threshold power as a function of temperature.

The QD lasers were grown on a high crystalline quality exact (001) GaAs-on-Si template incorporating no Ge related absorptive buffers [4]. A typical five-layer InAs/InGaAs dot-in-a-well (DWELL) structure was adopted as active region [5]. Transmission electron microscope (TEM) image of the complete as-grown structure and a schematic of the DWELL are shown in Fig. 1a and Fig. 1b, respectively. Effective defect trapping and reduction scheme through the V-grooved structure at the GaAs/Si hetero-interface (Fig. 1c) helps maintain good crystalline quality of the active device region (Fig. 1d). Microdisk cavities (Fig. 1e) were fabricated for rapid feedback of the

978-1-943580-23-1/17/$31.00 ©2017 Optical Society of America

QD performance and to promote high-quality factor and dense integration for short-reach communication links. The devices were characterized using micro-photoluminescence (μPL) in a surface-normal pump/collection configuration.

For 4-μm diameter micro-disks, lasing was achieved from 10 K up to room temperature under continuous wave optical pumping [6]. In 300 K, a distinct lasing peak appears at 1308 nm and increases sharply in intensity, signifying the transition from spontaneous emission to lasing (Fig. 1f). The smooth sidewall and vertical etching profile of the disk cavity (inset in Fig. 1f) lead to a low lasing threshold of around 200 μW and a high spontaneous emission coupling efficiency (β) of 10%. The β was extracted by fitting the S-shaped nonlinear characteristics (Fig. 1g) to a coupled rate equation model. Lasing was further evidenced through the pronounced narrowing of linewidth (inset in Fig. 1g). From 10 K to 300 K, lasing operation sustained with distinct kinks in the integrated output-power intensity versus the pump power (L–L) curve (Fig. 1h). The threshold pump power increases by a factor of ~2 as the temperature increases (inset in Fig. 1h), and the characteristic temperature T_0 was extracted to be around 105 K.

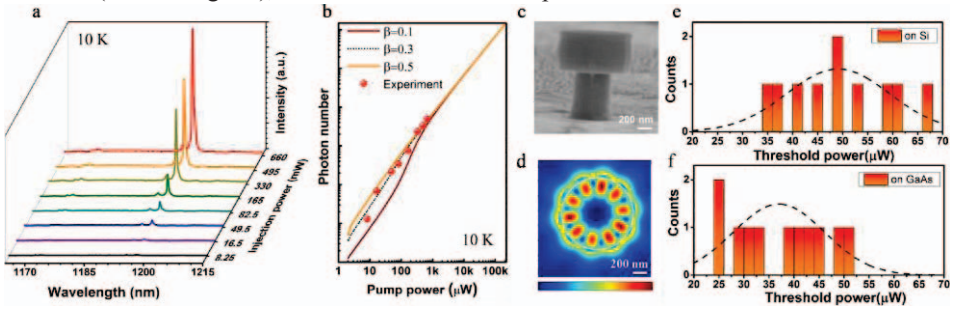

Fig. 2. (a) μPL spectra of the 1-μm-diameter microdisk laser at different pump powers at 10 K; (b) L-L curve in the log-log scale; (c) SEM image of the micro-disk; (d) simulated electric field distribution of the $TE_{1,5}$ resonance; (e) and (f) histograms of threshold schematic of the threshold for micro-disks on Si and GaAs.

For subwavelength micro-disk with diameter as small as 1-μm, lasing with low thresholds down to 35 μW has been demonstrated in the 1.2-μm wavelength range at 10 K (Fig. 2a) [7]. A high spontaneous emission factor was extracted to be 0.3 (Fig. 2b). The large β and small thresholds were attributed to the large ratio of quality factor over mode volume $Q/V_{eff} \approx 8600\ \mu m^{-3}$ in the ultra-small whispering gallery mode cavity (Fig. 2c). In Fig. 2d, the lasing mode was identified to be $TE_{1,5}$ according to finite-difference time-domain (FDTD) simulation. The micro-disk cavities were simultaneously fabricated on the GaAs-on-Si template and on a GaAs substrate with an identical cavity design for benchmarking. As shown in Fig. 2e and Fig. 2f, the average threshold for the micro-disk lasers on silicon (50 μW) compares favorably with the average value for lasers on the GaAs substrate (33 μW).

The optically-pumped microdisk lasers have shown that these quantum dot structures, grown heteroepitaxially on Si substrates, are excellent candidate sources for chip-scale Si-based photonics. This motivates our further exploration of approaches that allow for electrical injection of the QD gain material, coupled to index-matched silicon waveguide devices. While an ultimate goal would be electrical injection of the microdisk lasers, the sensitivity of the whispering gallery modes to the geometry of the contacts requires more detailed analysis and optimization of an integrative structure. Thus, we first set up a general framework that will allow for the integration of active and passive QD-on-silicon devices, using a Fabry–Pérot geometry for the QD lasers.

To do so, we designed a monolithic integration scheme that combines InAs quantum dots gain elements and index matched amorphous silicon waveguide devices. Typically, photoluminescence intensity degradation and wavelength shift occur for InAs QDs after high-temperature growth of a thick upper cladding layer, therefore restricting device performances [8]. To eliminate the above problem, we designed a thin-film low-temperature hydrogenated amorphous silicon (*a*-Si) waveguide for optical confinement. The *a*-Si has been tuned to achieve refractive index and mode-matched to III/V laser waveguides with smooth morphology and low optical loss. A schematic of the device is shown in Fig. 3a. The as-grown structure consists of a 50 nm *n*-GaAs contact layer, a 1.5 μm *n*-AlGaAs lower cladding layer, an un-doped InAs QDs active region, and a 50 nm *p*-GaAs contact layer. The laser cavity is defined by the PECVD deposited *a*-Si waveguide comprising of an *a*-Si core and a thin oxide buffer. Electrical confinement was attained by implanting both sides of the mesa with protons (H^+), which is also a low-temperature process without significant QD degradation. These implanted regions were electrically insulating so that current only flows through the center of the n-type mesa, realizing large electrical current overlap with the optical mode. Incident energy of 40 keV was chosen according to stopping and range of ions in matter (SRIM), such that the implanted region takes place right below the QDs active region. The implantation dose and proper annealing cycles were then optimized to achieve a high-resistivity implanted region with low-resistivity surface contact. Afterwards, mesas of 1.6 μm high were defined by standard optical lithography and wet chemical etching, followed

by oxide passivation and contact hole opening. Finally, Ti/Pt/Au *p*-metal contact was deposited on the *p*-GaAs layer and Ge/Au/Ni/Au *n*-metal contact was deposited on the *n*-GaAs layer for electroluminescence measurement. The measured forward biased current-voltage (*I-V*) characteristic and optical power-injection current (*L-I*) characteristics of the diode with a cavity length of 500 μm and a cavity width of 10 μm are shown in Fig. 3b. Electroluminescence centered at 1310 nm was observed (Fig. 3c).

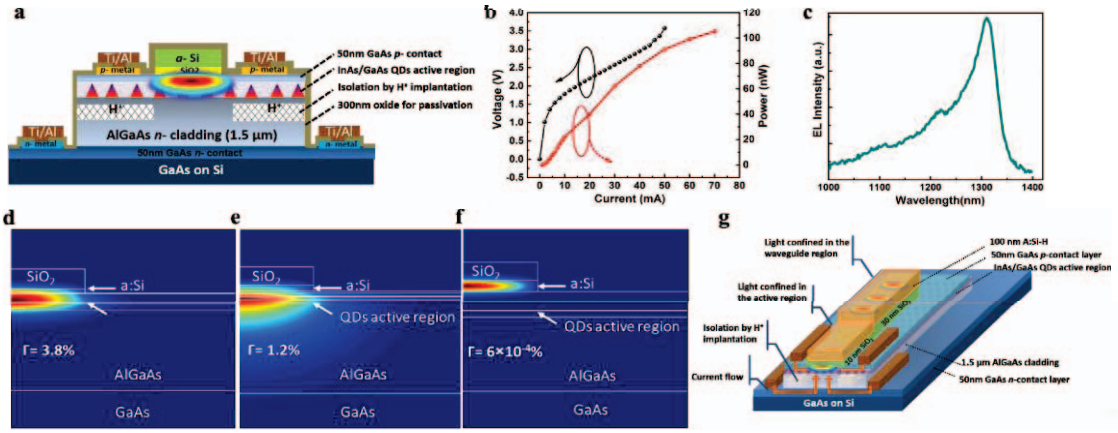

Fig. 3. (a) Schematics of the device structure; (b) Measured L-I and I-V curve; (c) EL spectrum; (d)-(f) simulated light confinement with different deposited material; (g) a proposed scheme to integrate laser and waveguide.

We further tuned the thickness of *a*-Si to modify its optical gain characteristics so that active and passive devices can be integrated. A 150 nm *a*-Si with a 20 nm oxide buffer contributes to a confinement factor of 3.8% in the QDs active region, suitable to achieve high modal gains in active devices, as shown in Fig. 3d. In this case, light evanescently overlaps both the QDs active region and the *a*-Si. The mode is thus electrically pumped from the III-V region while being guided by the *a*-Si waveguide. For the same thickness, *a*-Si with a thicker oxide buffer of 50 nm (Fig. 3e), the confinement factor in the QDs active region reduces to 1.2%, suitable for amplifiers with slightly lower modal gains to increase the saturation power. When both the *a*-Si core and oxide buffer are as thick as 300 nm, the mode is pulled more into the *a*-Si region and the confinement factor in the QDs active region reduces dramatically to 6e-6, as shown in Fig. 3f. Waveguides can thus be designed with the least modal gain to allow the propagation of light. This indicates the flexibility of designing different devices by managing the deposited thickness. A proposed scheme to integrate laser with waveguide utilizing different thicknesses of *a*-Si waveguide cladding is shown in Fig. 3g. Easy integration of both active and passive devices onto the same chip can be realized by tuning the thickness of PECVD deposited materials, eliminating the need for multiple epitaxial growths or elaborate device processing.

3. Conclusions

In conclusion, we demonstrate high performance InAs QDs lasers on exact (001) Si substrate. Room temperature lasing in a 4 μm disk as well as subwavelength lasing in a 1 μm disk has been demonstrated under continuous wave optical pumping. We further explore the possibility of forming a novel monolithic integration platform by combining the QDs gain elements and index matched a-Si waveguide. The integration scheme allows for independent optimization of III/V gain sections and the passive a-Si waveguides within a single photonic microchip.

4. References

[1] L. Di, and J. E. Bowers. "Recent progress in lasers on silicon." *Nat. Photon.* 4.8 (2010): 511-517.
[2] A. Y. Liu, *et al.* "Quantum dot lasers for silicon photonics." *Photon. Res.* **3,** B1-B9 (2015).
[3] S. Chen, *et al.* "Electrically pumped continuous-wave III-V quantum dot lasers on silicon." *Nat. Photon.* **10,** 307-311 (2016).
[4] A. Y. Liu, *et al.* "Electrically pumped continuous wave 1.3 μm quantum dot lasers epitaxially grown on on-axis (001) Si." *International Semiconductor Laser Conference (ISLC2016).*
[4] Qiang. Li, *et al*. "Growing antiphase-domain-free GaAs thin films out of highly ordered planar nanowire arrays on exact (001) silicon." *Appl. Phys. Lett* 106.7 (2015): 072105.
[5] A. Y. Liu, *et al.* "MBE growth of P-doped 1.3 μm InAs quantum dot lasers on silicon." *Journal of Vacuum Science & Technology B*, 32.2, 02C108 (2014).
[6] Y. Wan, *et al.* "Temperature characteristics of epitaxially grown InAs quantum dot micro-disk lasers on silicon for on-chip light sources," *Appl. Phys. Lett.* **109**, 011104 (2016).
[7] Y. Wan, *et al*. "Sub-wavelength InAs quantum dot micro-disk lasers epitaxially grown on exact Si (001) substrates." *Appl. Phys. Lett.* 108, 221101 (2016).
[8] G. Denis, *et al*. "Ground state lasing at 1.30 μm from InAs/GaAs quantum dot lasers grown by metal–organic chemical vapor deposition." *Nanotechnology* 21.10 (2010): 105604.).